

Fast magnetosonic modes of cylindrical magnetotail

I. S. Dmitrienko¹ ·

Abstract FMS modes are studied in the model of the magnetotail as a cylinder with plasma sheet. The presence of the plasma sheet leads to a significant modification of the modes existing in the magnetotail in the form of a cylinder with no plasma sheet. Azimuthal scales of the FMS modes differ significantly between the lobes and the plasma sheet. The azimuthal scale in the plasma sheet is much smaller than that in the magnetotail lobes. FMS waves with certain parameters are strongly reflected from the boundary between the lobes and the plasma sheet and are very weak in the plasma sheet.

1. Introduction

The magnetotail is affected by various perturbations originating from the environment it is surrounded by. Such perturbations can be transported by FMS waves across the magnetotail from areas of their origin. FMS waves deep in the magnetotail are mode converted into Alfvén waves, with the perturbation energy being further transferred along the magnetic field by Alfvén waves as disturbances of various spatial scales (Dmitrienko, 2013). When FMS waves are mode converted into Alfvén waves, accelerated plasma flows are formed (Dmitrienko, 2012); such flows can reach the surface of the planet. The Alfvén waves cause magnetic field perturbations and electron precipitations due to their longitudinal electric field (Watt & Rankin, 2010; Lysak & Song, 2003; Keiling *et al.*, 2005; Wright & Allan, 2008; Dmitrienko, 2010). Thus, FMS waves of the magnetotail are not only of interest as themselves but also in relation to the wide range of diverse phenomena resulting from their mode conversion into Alfvén waves.

Up until now the magnetotail FMS modes have been studied in very simple models only - either a cylindrical model without plasma sheet (McKenzie, 1970), or a flat model (Mills & Wright, 2000; Allan & Wright, 1998; Mazur *et al.*, 2010). Despite their simplicity, these models help capture some of the general features in FMS wave propagation in the magnetotail. The first of the two includes reflection of FMS waves propagating deep into the tail, while the second model reflects the existence of an FMS waveguide in the plasma sheet due to a strong inhomogeneity of the magnetotail parameters in the direction across the magnetotail. These results are, however, obtained in two different models, and either model is clearly not satisfactory. In this paper we address FMS modes in a model magnetotail taking into account both the nearly cylindrical shape of the magnetotail and the plasma sheet within.

¹ Institute of Solar-Terrestrial Physics SB RAS, Lermontov St. 126, Irkutsk 664033, Russia email: dmitrien@iszf.irk.ru

The current sheet, with strongly attenuating magnetic field inside, manifests itself as a strong inhomogeneity of the Alfvén velocity, in the FMS wave equations. Since the dispersion properties of FMS waves in the area of existence of the current sheet are determined by the sound velocity, whereas the value of the low Alfvén speed is insignificant, we neglect the presence of the current sheet and confine ourselves to including only the plasma sheet in the model.

We introduce a special orthogonal curvilinear coordinate system which generalizes the radial and azimuthal cylindrical coordinates for magnetotail cross-section. The boundary of the plasma sheet and lobes lies on the coordinate curves in this coordinate system. In this case it is possible to reduce the problem of describing the FMS modes to an ordinary second-order differential equation by using the "radial" WKB approximation. Together with the boundary conditions on the "azimuthal" coordinate, it gives a dispersion equation that determines the wave "radial" numbers as functions of "radial" coordinate.

2. Equations for FMS waves in cylindrical magnetotail with plasma sheet.

We assume that the magnetotail is a plasma column extended along the direction of magnetic field \mathbf{B}_0 ; this direction is chosen as the x coordinate of the Cartesian coordinate system. All unperturbed plasma parameters and the magnetic field are homogeneous with respect to this coordinate.

The homogeneity of the unperturbed parameters on x lets us consider a Fourier harmonic of the wave perturbation corresponding to this coordinate, i.e. suppose that the perturbation is the product of functions y and z by $\exp(ikz)$, where k is the longitudinal wave number. We will designate special orthogonal coordinates in the plane perpendicular to \mathbf{B}_0 as x^1, x^2 . We have $g_3 = 1, \partial_3 g_1 = \partial_3 g_2 = 0, B_{03} = B_0^3 = B_0$.

We will take linearized MHD equations:

$$\begin{aligned} \partial_t \mathbf{B} &= \nabla \times [\mathbf{v} \times \mathbf{B}_0], \\ m_i n_0 \partial_t \mathbf{v} &= \frac{1}{4\pi} [\nabla \times \mathbf{B}] \times \mathbf{B}_0 + \frac{1}{4\pi} [\nabla \times \mathbf{B}_0] \mathbf{B} - \nabla P, \\ \partial_t P + (\mathbf{v} \cdot \nabla) P_0 + V_s^2 \rho_0 \nabla \cdot \mathbf{v} &= 0, \\ \partial_t \rho + (\mathbf{v} \cdot \nabla) \rho_0 + \rho_0 \nabla \cdot \mathbf{v} &= 0. \end{aligned} \quad (1)$$

Here $\mathbf{B}, \mathbf{v}, \rho, P$ are magnetic field, velocity, density and pressure, respectively. Unperturbed parameters are subscripted with 0; V_s is sound velocity, $V_s = \sqrt{\frac{\gamma P_0}{\rho_0}}$, where γ is the adiabatic index.

We will designate the components of the field and velocity vectors in the plane perpendicular to the \mathbf{B}_0 as $B_{\perp k}, v_{\perp k}; k = 1, 2$.

Unperturbed parameters must satisfy the equations

$$\partial_k \left(\frac{B_0^2}{8\pi} + P_0 \right) = 0,$$

where $P_0 = P_0(x^1, x^2)$. We will put

$$P_0(x^1, x^2) = \overline{P} - \frac{B_0^2(x^1, x^2)}{8\pi}, \quad (2)$$

where $\overline{P} = \text{const}$.

Let us denote the perturbation of the full pressure as Ψ : $\Psi = \frac{1}{4\pi}B_0B_3 + P$. Taking into account (2) the equation for Ψ can be obtain from (1) in the form

$$\partial_1 \left(\sqrt{\frac{g_2}{g_1}} \frac{1}{B_0^2 l_a} \partial_1 \Psi \right) + \partial_2 \left(\sqrt{\frac{g_1}{g_2}} \frac{1}{B_0^2 l_a} \partial_2 \Psi \right) + \sqrt{g} \frac{1}{B_0^2 l_a} U \Psi = 0, \quad (3)$$

where $U = \frac{(\omega^2 V_a^{-2} - k^2)(\omega^2 c_s^{-2} - k^2)}{\omega^2 V_c^{-2} - k^2}$, and v_c is the velocity of slow magnetosonic wave, $V_c = \frac{c_s V_a}{\sqrt{(V_a^2 + c_s^2)}}$.

We will use the approximation of homogeneous plasma in a uniform field for the magnetotail lobes (its parts outside the plasma layer up to the outer boundary). We will index the unperturbed parameters of the lobes by the l subscript. The lobe plasma is cold ($\beta \ll 1$), therefore $V_{al}^2 \gg V_{sl}^2$ and we have $U = \omega^2 V_{al}^{-2} - k^2$. We will index the unperturbed parameters of the plasma sheet by the p -subscript. We will use the hot plasma approximation for the plasma sheet and confine ourselves to the homogeneous plasma and field approximation. When $\beta \gg 1$, therefore $V_{ap}^2 \ll V_{sp}^2$ and we have $U = \omega^2 V_{sp}^{-2} - k^2$. Thus strong inhomogeneity of the field in the current sheet is not important for U . We obtain

$$U = \begin{cases} \omega^2 V_{al}^{-2} - k^2, & \text{in the lobes} \\ \omega^2 V_{sp}^{-2} - k^2, & \text{in the plasma sheet} \end{cases}. \quad (4)$$

We have $\frac{B_{0l}^2}{8\pi} + P_{0l} = \frac{B_{0p}^2}{8\pi} + P_{0p}$ from (2). This equality can be replaced by the approximate equality $\frac{B_{0l}^2}{8\pi} = P_{0p}$ given the inequalities $B_{0l}^2 \gg B_{0ps}^2$ and $P_{0l} \ll P_{0p}$. Thus we have $V_{sp}^2 = V_{al}^2 \frac{\gamma \rho_{0l}}{2\rho_{0ps}}$ in (4).

Now let us specify the magnetotail cross section structure. We assume it to consist of a plasma layer shaped as a rectangle with sides $2h$ and $2R$ ($R > h$) and two lobes shaped as semicircles with radius R , their diameters adjacent to the longer side of the plasma layer. We define the coordinates in the plane as:

$$\rho = \begin{cases} |y|, & \text{when } |z| \leq h \\ \sqrt{y^2 + (|z| - h)^2}, & \text{when } |z| > h \end{cases}, \quad (5)$$

$$s = \begin{cases} z, & \text{when } -h \leq z \leq h, y > 0 \\ h + R \arccos \frac{y}{\sqrt{y^2 + (|z| - h)^2}}, & \text{when } z > h \\ -h - R \arccos \frac{y}{\sqrt{y^2 + (|z| - h)^2}}, & \text{when } z < -h \\ S - z, & \text{when } 0 < z \leq h, y < 0 \\ -S - z, & \text{when } 0 > z \geq -h, y < 0 \end{cases}. \quad (6)$$

Metric coefficients in the coordinate system : $x^1 = \rho$, $x^2 = s$ according to (5) and (6):

$$g_1 = 1, g_2 = \begin{cases} 1, & \text{for } -h \leq z \leq h \text{ (the plasma sheet)} \\ (\rho/R)^2, & \text{for } z > h \text{ and } z < -h \text{ (the lobes)} \end{cases}.$$

In the ρ, s coordinates, (3) takes the form

$$\frac{1}{\sqrt{g_2}} \partial_\rho (\sqrt{g_2} \partial_\rho \Psi) + \frac{1}{\sqrt{g_2}} B_0^2 l_a \partial_s \left(\frac{1}{\sqrt{g_2}} \frac{1}{B_0^2 l_a} \partial_s \Psi \right) + U \Psi = 0, \quad (7)$$

The parameters B_0 , ρ_0 have jumps as functions of s at the boundary of the plasma sheet and the lobes; g_2 has a jump as well.

The integration of (7) over s near the plasma sheet-lobes boundary gives conditions for matching the solution at this boundary as

$$\Psi(\bar{s} + 0) = \Psi(\bar{s} - 0), \quad (8)$$

$$\left[\frac{1}{\sqrt{g_2} B_0^2 l_a} \partial_s \Psi \right]_{(\bar{s}+0)} - \left[\frac{1}{\sqrt{g_2} B_0^2 l_a} \partial_s \Psi \right]_{(\bar{s}-0)} = 0, \quad (9)$$

where \bar{s} is one of the two values of s at the boundary given by the equations $s = \pm h$.

Outside the plasma sheet-lobe boundary, equation (7) takes the form

$$\frac{1}{\sqrt{g_2}} \partial_\rho (\sqrt{g_2} \partial_\rho \Psi) + \frac{1}{g_2} \partial_s \partial_s \Psi + U \Psi = 0. \quad (10)$$

We will use the WKB approximation to solve (10):

$$\Psi = \psi_+(\rho, s) \exp(i \int K d\rho) + \psi_-(\rho, s) \exp(-i \int K d\rho),$$

where K is a large wave number ($|K| \ll R^{-1}$), which gives a rapid change of Ψ in the ρ coordinate, while ψ_+ and ψ_- are slowly varying functions of ρ : $|\partial_\rho \psi_\pm / \psi_\pm| \ll |K|$. The + and - subscripts of ψ will be omitted.

We obtain from (10) in the main order of the WKB approximation:

$$\frac{1}{g_2} \partial_s \partial_s \psi + (U - K^2) \psi = 0. \quad (11)$$

Boundary conditions in the s coordinate are the periodicity conditions:

$$\psi(-S) = \psi(S), \quad \partial_s \psi(-S) = \partial_s \psi(S). \quad (12)$$

3. Dispersion equation for FMS modes.

Taking into consideration the symmetry with respect to $s = 0$ the periodicity conditions (12) on $[-S, +S]$ should be replaced by the following two boundary conditions within $[-S, 0]$:

$$\partial_s \psi(0) = 0, \quad \partial_s \psi(-S) = 0 \quad (13)$$

and

$$\psi(0) = 0, \quad \psi(-S) = 0. \quad (14)$$

Since there is symmetry on the $[-S, 0]$ with respect to $s = -S/2$ we can proceed further to the boundary conditions on $[-S, -S/2]$ and obtain:

$$\partial_s \psi(-S) = 0, \quad \partial_s \psi(-S/2) = 0, \quad (15)$$

$$\psi(-S) = 0, \quad \partial_s \psi(-S/2) = 0, \quad (16)$$

$$\partial_s \psi(-S) = 0, \quad \psi(-S/2) = 0, \quad (17)$$

$$\psi(-S) = 0, \quad \psi(-S/2) = 0, \quad (18)$$

instead of (13) and (14).

In the case of boundary conditions (15), we will seek the solution to (11) in the plasma sheet in the form

$$\psi = A \cos [Q_p (S + s)], \quad Q_p = \sqrt{U_p - K^2}, \quad U_p = \omega^2 V_{sp}^{-2} - k^2; \quad (19)$$

We will seek the solution in the lobes as

$$\psi = a \cos [Q_l (S/2 + s)], \quad Q_l = \frac{\rho}{R} \sqrt{U_l - K^2}, \quad U_l = \omega^2 V_{al}^{-2} - k^2. \quad (20)$$

These solutions satisfy (15) and we only have to match them at $s = -S + h$. To obtain the dispersion equation it is convenient to use the matching of the logarithmic derivative instead of (8), (9):

$$\left[\frac{1}{\sqrt{g_2} B_0^2 l_a} \frac{\partial_s \Psi}{\Psi} \right]_{(\bar{s}+0)} - \left[\frac{1}{\sqrt{g_2} B_0^2 l_a} \frac{\partial_s \Psi}{\Psi} \right]_{(\bar{s}-0)} = 0. \quad (21)$$

Substituting (19) and (20) in (21) we get

$$\tan [Q_l (-S/2 + h)] = \delta^{-1} \tan [Q_p h]. \quad (22)$$

We denoted $\delta = \frac{\sqrt{U_l - K^2} (B_0^2 l_a)_p}{\sqrt{U_p - K^2} (B_0^2 l_a)_l}$. The ratio of the mode amplitudes in the plasma sheet to those in the lobes is determined from (9):

$$\frac{A}{a} = \delta \frac{\sin [Q_l (-S/2 + h)]}{\sin [Q_p h]}. \quad (23)$$

The dispersion equation and the amplitude ratio for (16) - (18) are obtained similarly:

$$\tan [Q_l (-S/2 + h)] = -\delta^{-1} \tan^{-1} [Q_p h], \quad \frac{A}{a} = -\delta \frac{\sin [Q_l (-S/2 + h)]}{\cos [Q_p h]} \quad (24)$$

for (16),

$$\tan [Q_l (-S/2 + h)] = -\delta \tan^{-1} [Q_p h], \quad \frac{A}{a} = -\delta \frac{\cos [Q_l (-S/2 + h)]}{\sin [Q_p h]} \quad (25)$$

for (17),

$$\tan [Q_l (-S/2 + h)] = \delta \tan [Q_p h], \quad \frac{A}{a} = \delta \frac{\cos [Q_l (-S/2 + h)]}{\cos [Q_p h]} \quad (26)$$

for (18).

It is easy to see that when $\delta \rightarrow \infty$ we generally get values of the order of 1 for A/a from (23) - (26). This means that the amplitudes of the modes in the plasma sheet and in the lobes are values of the same order for large values of δ .

When $\delta \rightarrow 0$ it follows from (23)-(26) that $\frac{A}{a} \sim \delta$. A small ratio $\frac{A}{a}$ means that for small δ the modes are almost not present in the plasma sheet and are concentrated

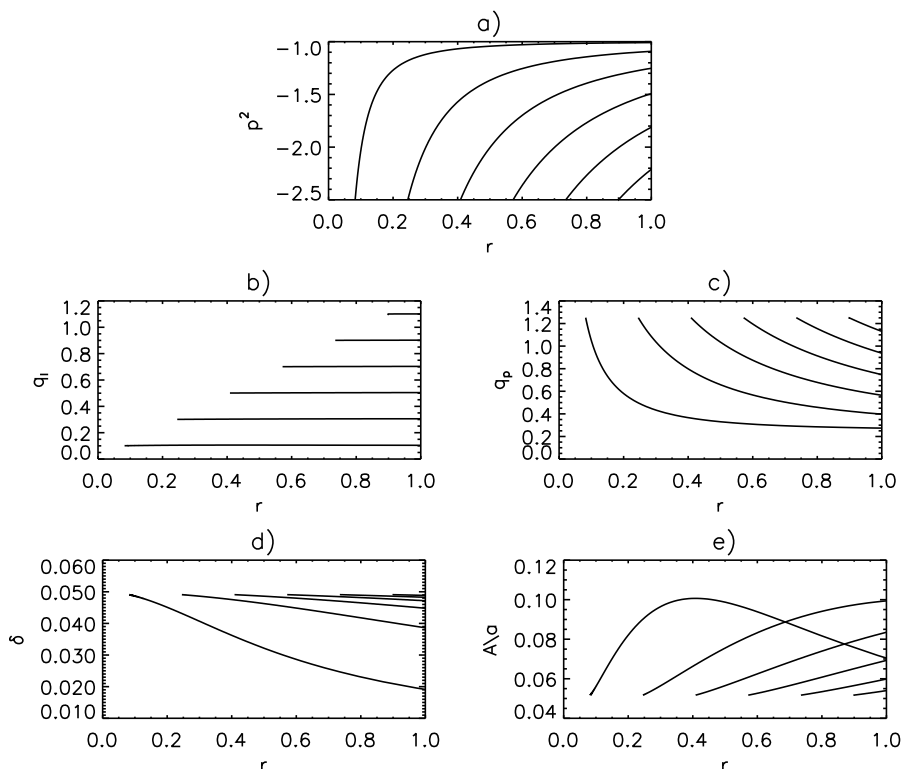


Figure 1. Plots of numerically calculated $p^2(r)$, $q_l(r)$, $q_p(r)$, $\delta(r)$, $\frac{A}{a}(r)$ when $h/R = 0.1, b = 0.1, \lambda = 0.05, w = 0.05, t = 10, v = 0.05$.

in the magnetotail lobes. This means that the FMS modes propagating in the lobes are strongly reflected from their boundary with the plasma sheet.

The results of numerical calculations of the eigenvalues $p^2(r)$ and the corresponding ratio of the amplitudes as well as $q_p(r)$, $q_l(r)$ and $\delta(r)$ for (22) are shown in Fig. 1. Fig. 1 is the case of parameters for which the modes decay from the magnetotail boundary deeper into the magnetotail. Fig. 1a shows $p^2(r)$, while Fig. 1b and 1c show wave numbers $q_p(r)$ and $q_l(r)$ corresponding to the coordinate s . We see in figures 1b and 1c that azimuthal scales of the modes are substantially smaller in the plasma sheet than those in the lobes. Fig. 1d depicts $\delta(r)$. As we can see, δ is small. The curves in Fig. 1d show that the modes are mainly concentrated in the magnetotail lobes.

4. Conclusions

A model of the magnetotail is proposed taking into account both its external structure and the presence of a plasma sheet within. A special system of coordinates is introduced corresponding to such a model. Dispersion equations for FMS modes are derived using the model and the coordinates introduced. It is shown that the

azimuthal scales of FMS modes are substantially different between the lobes and the plasma sheet - the azimuthal scale in the plasma sheet is much smaller than that in the magnetotail lobes; the mode amplitude distributions in the azimuthal coordinate are inhomogeneous. The FMS waves decaying deep into the magnetotail but propagating along the azimuth coordinate are primarily concentrated in the lobes and weakly penetrate into the plasma sheet.

References

- ALLAN, W. & WRIGHT, N. 1998 Hydromagnetic wave propagation and coupling in a magnetotail waveguide. *J. Geophys. Res.* **103**, No. A2, 2359–2368, DOI:10.1029/97JA02874.
- DMITRIENKO, I. S. 2013 Evolution of FMS and Alfvén waves produced by the initial disturbance in the FMS waveguide. *J. Plasma Physics* **79**, 7–17, doi:10.1017/S0022377812000608.
- DMITRIENKO, I. S. 2012 Formation of accelerated ion flows in Alfvén disturbances of the magnetotail. *J. Geomagnetism and Aeronomy* **51**, Issue 8, 1160, doi:10.1134/S0016793211080032.
- DMITRIENKO, I. S. 2010 Spatio-temporal evolution of thin Alfvén resonance layer. *J. Plasma Physics* **76**, 709, doi:10.1017/S002237781000022X.
- KEILING, A., PARKS, G. K., WYGANT, J. R., DOMBECK, J., MOZER, F. S., RUSSELL, C. T., STRELTSOV, A. V. & LOTKO, W. 2005 Some properties of Alfvén waves: Observations in the tail lobes and the plasma sheet boundary layer. *J. Geophys. Res.* **110**, No. A10, COA 6-1, A10S11, DOI:10.1029/2004JA010907.
- LYSAK, R. L. & SONG, Y. 2003 Kinetic theory of the Alfvén wave acceleration of auroral electrons. *J. Geophys. Res.* **108**, No. A4, COA 6-1,8005, DOI:10.1029/2002JA009406.
- MAZUR, N. G., FEDOROV, E. N. & PILIPENKO, V. A. 2010 MHD Waveguides in Space Plasma. *Plasma Phys. Rep.* **36**, No. 7, 609–626, DOI:10.1134/S1063780X10070081.
- MCKENZIE, J. F. 1970 Hydromagnetic oscillations of the geomagnetic tail and plasma sheet. *J. Geophys. Res.* **75**, No. 28, 5331–5339, DOI:10.1029/JA075i028p05331.
- MILLS, K. J. & WRIGHT, A. N. 2000 Trapping and excitation of modes in the magnetotail. *Physics of Plasmas* **7**, No. 5, 1572–1581, DOI:10.1063/1.873977.
- WATT, C. E. J., & RANKIN, R. 2010 Do magnetospheric shear Alfvén waves generate sufficient electron energy flux to power the aurora? *J. Geophys. Res.* **115**, No. A7, A07224, doi:10.1029/2009JA015185.
- WRIGHT, A. N., & ALLAN, W. 2008 Simulations of Alfvén waves in the geomagnetic tail and their auroral signatures. *J. Geophys. Res.* **113**, No. A2, A02206, DOI:10.1029/2007JA012464.

